Photooxidation of Cytochrome b_{559} in Oxygen-Evolving Photosystem II†

Carolyn A. Buser,‡ Bruce A. Diner,§ and Gary W. Brudvig*,‡

Department of Chemistry, Yale University, New Haven, Connecticut 06511, and Central Research & Development Department, E. I. Du Pont de Nemours & Co., Wilmington, Delaware 19880-0173

Received March 13, 1992; Revised Manuscript Received August 14, 1992

ABSTRACT: Cytochrome b_{559} (cyt b_{559}) is an intrinsic and essential component of the photosystem II (PSII) protein complex, but its function, stoichiometry, and electron-transfer kinetics in the physiological system are not well-defined. In this study, we have used flash-detection optical spectroscopy to measure the kinetics and yields of photooxidation and dark reduction of cyt b_{559} in untreated, O_2-evolving PSII-enriched membranes at room temperature. The dark redox states of cyt b_{559} and the primary electron acceptor, Q_A, were determined over the pH range 5.0–8.5. Both the fraction of dark-oxidized cyt b_{559} and dark-reduced Q_A increased with increasing acidity. Consistent with these results, an acid-induced drop in pH from 8.5 to 4.9 in a dark-adapted sample caused the oxidation of cyt b_{559}, indicating a shift in the redox state during the dark reequilibration. As expected from the dark redox state of cyt b_{559}, the rate and extent of photooxidation of cyt b_{559} during continuous illumination decreased toward more acidic pH values. After a single, saturating flash, the rate of photooxidation of cyt b_{559} was of the same order of magnitude as the rate of $S_2\,Q_A^-$ charge recombination. In untreated PSII samples at pH 8.0 with 42% of cyt b_{559} oxidized and 15% of Q_A reduced in the dark, 4.7% of one copy of cyt b_{559} was photooxidized after one flash with a $t_{1/2}$ of 540 ± 90 ms. On the basis of our previous work [Buser, C. A., Thompson, L. K., Diner, B. A., & Brudvig, G. W (1990) *Biochemistry 29*, 8977] and the data presented here, we conclude that S_{n+1}, $Y_Z^{\bullet}$, and $P680^+$ are in redox equilibrium and cyt b_{559} (and Y_D) are oxidized via $P680^+$. After a period of illumination sufficient to fully reduce the plastoquinone pool, we also observed the pH-dependent dark reduction of photooxidized cyt b_{559}, where the rate of reduction decreased with decreasing pH and was not observed at pH <6.4. To determine the direct source of reductant to oxidized cyt b_{559}, we studied the dark reduction of cyt b_{559} and the reduction of the PQ pool as a function of 3-(3,4-dichlorophenyl)-1,1-dimethylurea (DCMU) concentration. We find that DCMU inhibits the reduction of cyt b_{559} under conditions where the plastoquinone pool and Q_A are reduced. We conclude that $Q_B^{-\bullet}(H^+)$ or Q_BH_2 is the most likely source of the electron required for the reduction of oxidized cyt b_{559}. On the basis of our results and their mechanistic implications, we suggest that cyt b_{559} mediates cyclic electron transfer within PSII, where cyt b_{559} is oxidized by $P680^+$ via a monomer chlorophyll and is reduced by a reducing equivalent from the Q_B site.

Cytochrome b_{559} (cyt b_{559}) is closely associated with the reaction center of PSII[1] and has long been the object of experimental scrutiny. However, its function and stoichiometry remain controversial. The oxidation and reduction of cyt b_{559} by the light-induced reactions in PSII suggest a functional role for cyt b_{559} in the redox chemistry of the reaction center. However, the low quantum yields of these reactions exclude a role for cyt b_{559} in the main electron transport chain. Furthermore, the two polypeptides (α and β) associated with the cyt b_{559} protein appear to have a significant structural role, since the presence of the β-polypeptide is required for the assembly of the PSII reaction center (Pakrasi et al., 1990). As an intrinsic, redox-active component of the PSII reaction center, cyt b_{559} may have a function related to the unique ability of PSII to oxidize water, such as a role in the protection of the reaction center from the highly oxidizing environment generated in PSII for the catalyzed oxidation of water (Thompson & Brudvig, 1988). In order to fully understand electron transport and water oxidation in PSII, it is essential to characterize the paths and kinetics of oxidation and reduction of cyt b_{559} in O_2-evolving PSII.

Both in O_2-evolving and in non-O_2-evolving PSII, the dominant path of reduction of $P680^+$ occurs via the oxidation of the tyrosine residue Y_Z (Scheme I). In untreated O_2-evolving chloroplast and PSII-enriched membranes, the rate of electron transfer from Y_Z to $P680^+$ is several orders of magnitude faster than the rate of electron donation from cyt b_{559} to $P680^+$. As a result, the quantum yield of oxidation of cyt b_{559} by P_{680}^+ is very low in comparison to the quantum yield for formation of $Y_Z^{\bullet}$ per reaction center turnover [reviewed by Mathis and Rutherford (1987)]. Consequently, earlier studies have characterized the photooxidation of cyt b_{559} only under conditions in which the electron donation from the Mn complex is either prevented or circumvented; inactivation of the O_2-evolving complex significantly slows Y_Z to $P680^+$ electron-donation kinetics [Conjeaud & Mathis, 1980; reviewed by Buser et al. (1990)]. Whereas the small extent and slow rate of oxidation of cyt b_{559} are incompatible with its involvement in the dominant path of electron transfer, the kinetics and yield are suggestive of a competition between cyt b_{559} and the water-oxidizing path for electron donation to $P680^+$.

† This work was supported by the National Institutes of Health (GM 32715).

‡ Yale University.

§ E. I. Du Pont de Nemours & Co.

[1] Abbreviations: BBY-type PSII, PSII prepared by the method of Berthold, Babcock, and Yocum (1981); bicine, *N,N*-bis(2-hydroxyethyl)-glycine; Chl, chlorophyll; Chl_z, monomer chlorophyll involved in photooxidation of cytochrome b_{559}; cyt, cytochrome; DCMU, 3-(3,4-dichlorophenyl)-1,1-dimethylurea; EPR, electron paramagnetic resonance; Hepes, *N*-(2-hydroxyethyl)piperazine-*N*′-2-ethanesulfonic acid; MES, 2-(*N*-morpholino)ethanesulfonic acid; PQ, plastoquinone; PQH_2, plastoquinol; PSII, photosystem II; tricine, *N*-[tris(hydroxymethyl)methyl]-glycine.

0006-2960/92/0431-11449$03.00/0 © 1992 American Chemical Society

Scheme I: Pathways for Electron Donation to $P680^+$ in O_2-Evolving PSII

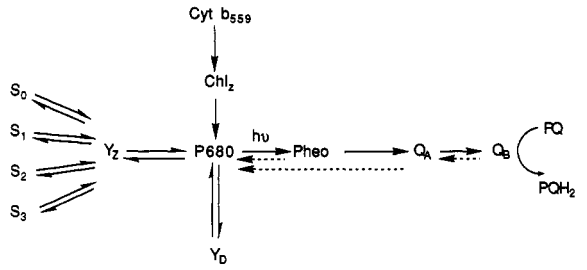

In earlier work, we studied the kinetics and yields of photooxidation of cyt b_{559} in O_2-inactive, NH_2OH-treated PSII-enriched membranes at room temperature (Buser et al., 1990). In dark-adapted, O_2-inactive PSII-enriched membranes, in which ≈20% of cyt b_{559} was oxidized and ≈52–64% of Q_A was reduced in the dark, we observed the photooxidation of 3.5–4.7% of cyt b_{559} after a single, saturating flash with a $t_{1/2} \approx 13$ ms (pH 6.2).[2] The BBY-type preparation of these PSII samples slows Q_A to Q_B electron transfer (by reducing the size of the PQ pool or possibly by damaging the Q_B site). The subsequent NH_2OH treatment removes the tetranuclear Mn complex of the O_2-evolving center and appears to completely inhibit Q_A to Q_B electron transfer (either by further depletion or reduction of the PQ pool during the NH_2OH treatment). As a result, the charge-separated state $Y_Z^{\bullet}\ Q_A^-$ has a lifetime of >1 ms in NH_2OH-treated PSII-enriched membranes. On the basis of our results and earlier investigations of electron transfer in O_2-inactive PSII, we proposed a model for electron donation in which $Y_Z^{\bullet}$ and $P680^+$ are in redox equilibrium and cyt b_{559} and Y_D are oxidized via $P680^+$ during the lifetime of the oxidizing equivalent on $Y_Z/P680$ (i.e., the lifetime of the $Y_Z^{\bullet}\ Q_A^-$ charge separation). On the basis of the success of this model to describe the electron-transfer events in O_2-inactive PSII reaction centers, we suggested that, in O_2-active PSII, S_{n+1}, $Y_Z^{\bullet}$, and $P680^+$ are in redox equilibrium (Scheme I) and predicted that the kinetics and yields of electron donation from cyt b_{559} and Y_D to $P680^+$ will depend on the lifetime of the oxidizing equivalent on $S_n/Y_Z/P680$.

The photoreduction, as well as the photooxidation, of cyt b_{559} has been observed in PSII-enriched membranes and chloroplasts; however, the kinetics of reduction are not well characterized and the identification of the reductant species to cyt b_{559} remains ambiguous. Comparison of the kinetics of reduction of cyt b_{559} and the PQ pool in chloroplasts led to the general conclusion that cyt b_{559} is reduced by either Q_A, Q_B, or plastoquinone (Cramer & Whitmarsh, 1977). Since then, several studies, using a variety of inhibitors to block Q_A to Q_B electron-transfer or to inhibit either the oxidation or reduction of the PQ pool, have attempted to further pinpoint the reductant of oxidized cyt b_{559}. Although these studies generally identify either the Q_B site or the PQ pool as the source of electrons to cyt b_{559}, the results are inconsistent. For example, the inhibitor DCMU has been reported to completely inhibit photoreduction (Tsujimoto & Arnon, 1985), to partially inhibit photoreduction (Yamagishi & Fork, 1987), to only affect the rate but not the extent of photoreduction (Whitmarsh & Cramer, 1978), or to be necessary to detect the photoreduction of cyt b_{559} at room temperature (Ben-Hayyim, 1984). Recently, the photoreduction of cyt b_{559} in thylakoids was reinvestigated, where the rate and extent of cyt b_{559} photooxidation were compared to the rate of electron transport from water to methyl viologen as a function of DCMU concentration (Samson & Fork, 1991). Since DCMU concentrations which appeared to block the photoreduction of methyl viologen were found to only partially inhibit the rate of cyt b_{559} photoreduction, the authors suggest reduced Q_A as the reductant to cyt b_{559}. However, in addition to difficulty of deconvoluting the cyt b_{559} absorbance spectrum from cyt b_6 and cyt f in thylakoids, the presence of ferricyanide in their assay of electron transfer may have short-circuited the methyl viologen acceptor, resulting in an underestimation of electron transfer through the Q_B site.

In past studies, another complication in the determination of the oxidative and reductive path for cyt b_{559} and the assignment of its functional role was the ambiguity of its stoichiometry in both chloroplasts and PSII-enriched membranes. Using EPR and differential absorbance spectroscopy and employing both internal and external standards for the quantitation of cyt b_{559}, we have found a 1:1 stoichiometry of cyt b_{559} per PSII reaction center in BBY-type PSII preparations (Buser et al., 1992).

In this study, we report the first kinetic and yield-per-flash measurements of the photooxidation and dark reduction of cyt b_{559} obtained with *O_2-evolving* PSII-enriched membranes. Using flash-detection optical spectroscopy, we have investigated the dark redox state of cyt b_{559}, the kinetics of cyt b_{559} photooxidation during continuous illumination and after a single, saturating flash, and the kinetics of dark reduction of cyt b_{559}, all as a function of pH. To elucidate the mechanism of oxidation of cyt b_{559}, we measured the rate of cyt b_{559} photooxidation and $S_2\ Q_A^-$ recombination over the pH 5–8.6 range in DCMU-treated PSII. Finally, in an effort to identify the reductant of cyt b_{559}, we compared the rate of dark reduction of cyt b_{559} at different DCMU concentrations in the presence of a reduced plastoquinone pool.

MATERIALS AND METHODS

PSII-enriched membranes were isolated from market spinach leaves by a modified version (Beck et al., 1985) of the isolation procedure described by Berthold et al. (1981). The Chl concentration was determined by the method of Arnon et al. (1949). Prior to the optical and EPR studies, the PSII-enriched membranes were stored at a Chl concentration of 4–8 mg of Chl/mL in resuspension buffer [15 mM NaCl, 20 mM MES, and 30% (v/v) ethylene glycol at pH 6.0] at 77 K. The sample preparation and spectroscopic data of the NH_2OH-treated PSII-enriched membranes presented in this paper are discussed in detail in the Materials and Methods and Results of the study by Buser et al. (1990). The yield of photooxidation of cyt b_{559} in NH_2OH-treated PSII was reanalyzed, assuming 175 ± 25 Chl molecules per reaction center.

The PSII-enriched membranes exhibited O_2-evolution activities of 300–400 μmol of O_2/(mg of Chl·h). The ratio of Chl to reaction center was determined by the EPR signal II_s ($Y_D^{\bullet}$) spin quantitation procedure described by Babcock et al. (1983), with potassium nitrosodisulfonate (Aldrich) as the spin standard. This assay assumes a stoichiometry of one Y_D per PSII reaction center and the complete oxidation of Y_D after a 20-min, 273 K illumination period. The continuous illumination period was followed by a 1-min, 273 K dark-

[2] Previously, we miscalculated the fraction of cyt b_{559} photooxidized in NH_2OH-treated PSII-enriched membranes by a logarithmic factor of 2.303 and by an overestimation of the number of Chl per reaction center in NH_2OH-treated PSII-enriched membranes (Buser et al., 1990). In the calculations in this paper, we have assumed 175 ± 25 Chl per NH_2-OH-treated PSII reaction center.

adaption period to allow for the complete reduction of $Y_Z^{\bullet}$ prior to the EPR measurement of $Y_D^{\bullet}$ at 15 K. In the PSII preparations used in this study, we have obtained values ranging from 165 to 230 Chl per PSII reaction center.

For the optical studies at varied pH, buffer solutions consisting of 15 mM NaCl, 20 mM buffer (MES for pH 6.0 and 6.5, Hepes for pH 7.0 and 7.5, tricine for pH 8.0, and bicine for pH 8.3 and 8.6), and 30% (v/v) ethylene glycol were prepared and adjusted to the desired pH with NaOH. All samples were used within a 2-h interval of equilibration to 25 °C and dilution with buffer at any given pH to a concentration of 0.02–0.06 mg of Chl/mL. After dilution, the samples were regularly monitored for decay by a measurement of the maximum absorbance change at 560 nm during continuous illumination. Although some variability in the amount of light scattering was observed from one PSII preparation to another, all preparations behaved very similarly and gave rise to the same absorbance changes. After each set of measurements, the Chl concentration and pH of the sample were measured. All absorbance measurements were normalized to a Chl concentration of 0.060 mg of Chl/mL. The concentrations of cyt b_{559}, Q_A, and the PQ pool were calculated from the amplitude of their respective light-induced absorbance changes, the differential extinction coefficient, and the EPR-determined Chl per PSII ratio for a given sample: $\Delta\epsilon = 17.5$ mM^{-1} cm^{-1} at 560–570 nm for cyt b_{559}(red–ox), $\Delta\epsilon = 13$ mM^{-1} cm^{-1} at 325 for Q_A^-–Q_A, and $\Delta\epsilon = 13$ mM^{-1} cm^{-1} at 263 nm for PQH_2–PQ (Cramer et al., 1986; van Gorkom, 1974b; Amesz, 1973).

Optical absorbance measurements were performed at 25 °C on a flash-detection spectrophotometer similar to that described by Joliot et al. (1980). Continuous illumination was provided by a cluster of four light-emitting diodes (Toshiba TLRA 150C, λ_{max} = 650 nm). Saturating actinic flashes were provided by a dye laser (Candela Co. Model SLL-250, 600-ns total duration, dye Oxazine 720, λ_{max} = 699 nm). The absorbance changes at a given wavelength were monitored by a series of probe flashes (EG&G Model FX-199U) filtered through the monochromator (HL, Jobin-Yvon). Fluorescence yield measurements of Chl in PSII were measured in the flash-detection spectrophotometer using a xenon actinic flash (EG&G Model FX-199) filtered by an infrared reflecting filter (MTO Atherex TA2), a Corning 4-96, and a Kodak Wratten 34. The fluorescence yield was monitored with probe flashes at 422 nm. The probe flashes used in the absorbance and fluorescence measurements did not contribute significantly to light-driven electron transfer.

The kinetic data of the photooxidation and reduction of cyt b_{559} and reoxidation of Q_A were analyzed with a single-exponential or biexponential curve-fitting routine of the Macintosh KaleidaGraph 2.1.2 program, using a Marquardt algorithm (see text and figure legends for further details).

RESULTS

Determination of the Dark Redox State of Cyt b_{559} in O_2-Evolving PSII-Enriched Membranes. To determine the dark redox state of cyt b_{559} in O_2-evolving PSII-enriched membranes, we measured the absorbance change of the α-band of cyt b_{559} in oxidized (ferricyanide) minus reduced (dark-adapted, ascorbate-treated, and sodium borohydride-treated) difference spectra, as shown in Figure 1a. The peak at 560 nm and the 10-nm width at half-height of the oxidized minus reduced difference spectra are in good agreement with the peak and width observed for light-induced cyt b_{559} oxidation in the double-mutant S56 of the green alga *Chlorella sorokiniana* (Lavergne, 1987) and in NH_2OH-treated PSII-enriched membranes (Buser et al., 1990).

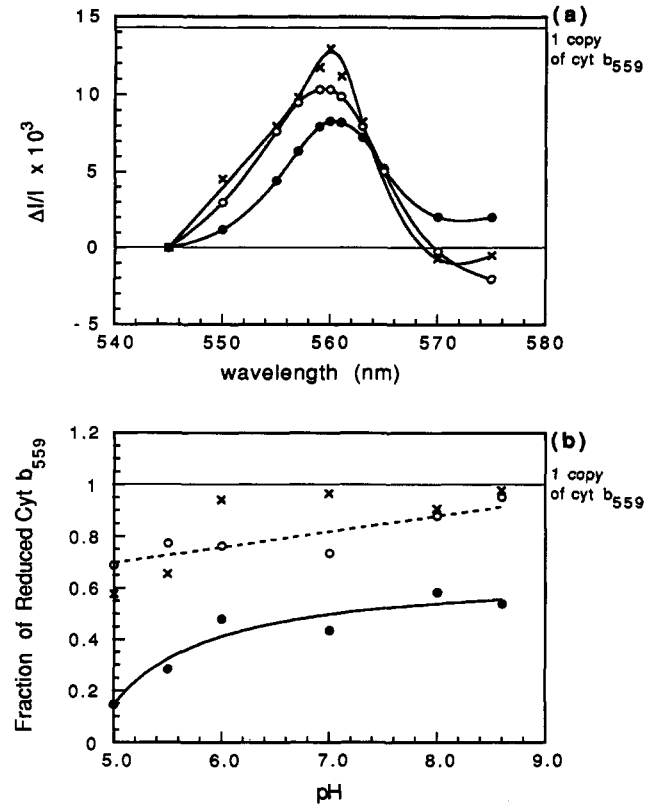

FIGURE 1: (a) Ferricyanide oxidized minus reduced difference spectrum of dark-adapted, untreated BBY-type PSII-enriched membranes (●), after the addition of 2 mM ascorbate (○), and after the further addition of $NaBH_4$ (solid) (×) at pH 7.0. (b) pH dependence of the dark redox state of cyt b_{559} in BBY-type PSII-enriched membranes. The measurement in (a) was repeated over the pH range 5.0–8.6. The fraction of reduced cyt b_{559} was calculated from the 560–570-nm absorbance difference in dark-adapted (●, —), ascorbate- (2 mM) treated (○, - - -), and ascorbate plus $NaBH_4$- (solid) treated (×) at each pH [$\Delta\epsilon$ (560–570 nm) = 17.5 mM^{-1} cm^{-1} and 190 Chl per reaction center].

Repeating the same measurement as in Figure 1a for the pH range 5.0–8.6, we subsequently calculated the fraction of dark-reduced cyt b_{559} from the 560–570-nm absorbance change in dark-adapted, ascorbate-reduced and sodium borohydride-reduced PSII samples; the results are shown in Figure 1b. Quantitation of the pH dependence of the dark redox state of cyt b_{559} indicates that in O_2-evolving PSII-enriched membranes, devoid of cytochromes *f* and b_6, approximately 85% and 46% of cyt b_{559} are oxidized in the dark at pH 5.0 and 8.6, respectively. In agreement with our previous results (Buser et al., 1992), the fully oxidized (ferricyanide) minus completely reduced (ascorbate plus sodium borohydride) difference spectra for the pH range of 6.0–8.6 correspond to a stoichiometry of one cyt b_{559} per reaction center. At pH < 6, the addition of sodium borohydride resulted in a significant distortion in the baseline. Therefore, the quantitation at low pH in the presence of sodium borohydride is less reliable. Most likely, cyt b_{559} is completely reduced by sodium borohydride at pH 5–6 (Figure 1b), since further addition of sodium dithionite did not induce additional reduction (data not shown).

Steady-State Photooxidation and Dark Reduction of Cyt b_{559} in O_2-Evolving PSII-Enriched Membranes. Figure 2 shows the visible absorbance spectrum observed after 6 s of continuous illumination of dark-adapted PSII-enriched membranes at pH 8.0 and room temperature. As in Figure 1a, the characteristic peak at 560 nm and the 10-nm width at half-height in the difference spectrum of Figure 2 are in agreement with previously published spectra for cyt b_{559}.

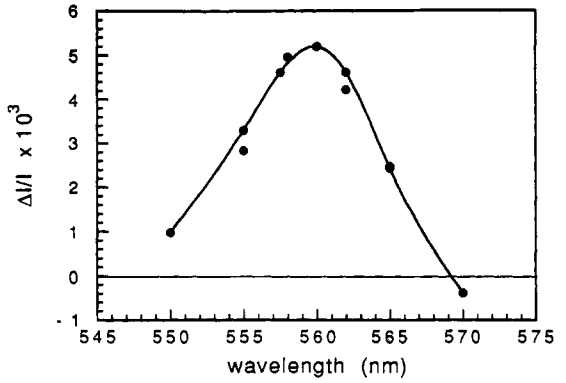

FIGURE 2: Red-visible spectrum of the light-induced absorbance change after 6 s of continuous illumination of dark-adapted PSII-enriched membranes at pH 8.0. At 560 nm, the absorbance change after 6 s of continuous illumination is 90% of the maximum absorbance observed after 21 s of continuous illumination.

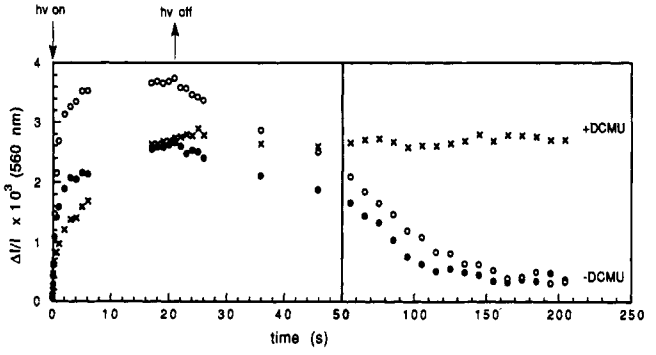

FIGURE 3: Time course of the light-induced absorbance change at 560 nm in dark-adapted (●), preilluminated (○), and preilluminated and subsequently DCMU- (20 μM) treated (×) PSII-enriched membranes at pH 8.0. Preillumination consisted of 21 s of continuous illumination followed by 3 min of dark adaption prior to the second illumination. DCMU was added at the end of the 3-min dark-adaption period, and the sample was allowed to incubate for 1 min in the dark prior to the measurement.

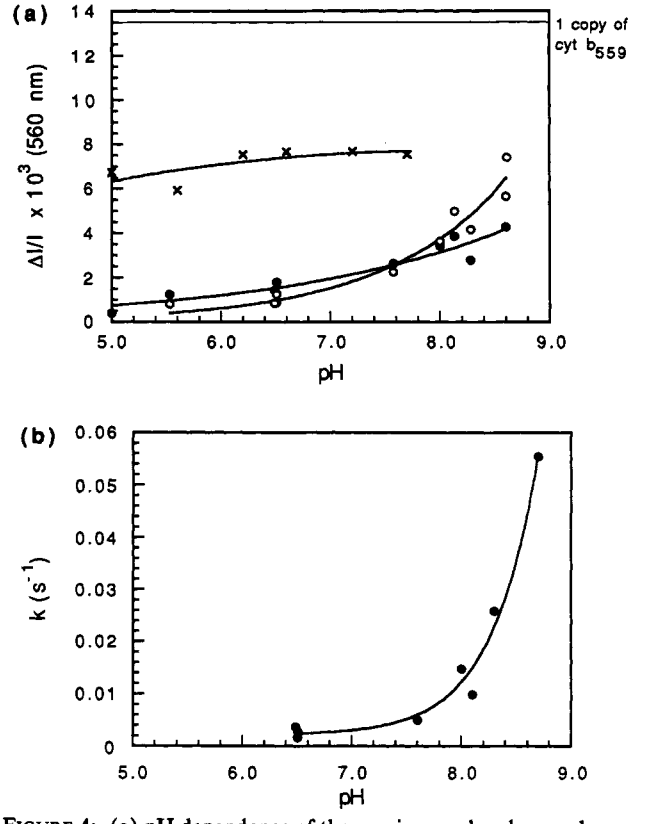

FIGURE 4: (a) pH dependence of the maximum absorbance change observed at 560 nm during continuous illumination of dark-adapted (●) and preilluminated (○) PSII-enriched membranes and dark-adapted, NH_2OH-treated (×) PSII-enriched membranes. The same preillumination was used as in Figure 3. The horizontal solid line at $\Delta I/I \times 10^3 = 13.4$ corresponds to the expected oxidized minus reduced absorbance difference of one copy of cyt b_{559} [$\Delta\epsilon$ (560–570 nm) = 17.5 mM^{-1} cm^{-1} and 200 Chl per reaction center]. (b) pH dependence of the rate of the dark reduction of cyt b_{559} in PSII-enriched membranes during the dark period following 21 s of continuous illumination. The kinetics of reduction of photooxidzed cyt b_{559} were calculated from a single-exponential curve fit to the time course of the absorbance change at 560 nm upon cessation of illumination.

To characterize the photoinduced reactions of cyt b_{559}, we first measured the light-induced absorbance changes at 560 nm in dark-adapted and preilluminated PSII-enriched membranes in the absence and presence of DCMU. Figure 3 shows the photooxidation and dark reduction of cyt b_{559} in dark-adapted, preilluminated, and preilluminated and subsequently DCMU-treated PSII samples at pH 8.0. Two significant observations from Figure 3 are the DCMU-induced inhibition of the dark reduction of cyt b_{559} (discussed later) and the increase in the yield of photooxidation of cyt b_{559} at pH 8.0 after an initial preillumination period. The latter result suggests that, at basic pH, both the photooxidized and a fraction of the dark-oxidized cyt b_{559} are reduced during the 3-min dark-adaption period after preillumination. More explicitly, the reducing equivalents on the acceptor side, formed via the oxidation of water during continuous illumination, are in excess with respect to cyt b_{559}^{ox} after preillumination, and more reduced cyt b_{559} is formed than was present prior to the first illumination.

The maximum yield of photooxidation of cyt b_{559} in O_2-active PSII during continuous illumination, shown in Figure 4a, displays a significant pH dependence, which, in part, reflects the pH dependence of the dark redox state of cyt b_{559} (Figure 1b). Emphasizing the result shown in Figure 3, a larger fraction of cyt b_{559} is photooxidized during a second illumination at basic pH (following a 21-s preillumination and 3-min dark adaption period); in contrast, at neutral and acidic pH, a lesser fraction of cyt b_{559} is photooxidized during a second illumination. This pH-dependent effect on the amount of photooxidizable cyt b_{559} in dark-adapted versus preilluminated samples suggests that the dark reduction pathway of photooxidized cyt b_{559} is inhibited at acidic pH. Consistent with this interpretation is the pH dependence of the rate of dark reduction of cyt b_{559} after illumination, shown in Figure 4b. The rate and extent of reduction of photooxidized cyt b_{559} in the dark decreases toward more acidic pH and appears to be completely blocked below about pH 6. Probably one consequence of this apparent inhibition of reduction of photooxidized cyt b_{559} at pH $\leq$ 6 is the increasing fraction of dark-oxidized cyt b_{559} at acidic pH (Figure 1b).

Dark Redox State of Q_A: Determination of the Extinction Coefficient for the C550 Measurement in PSII. To obtain some insight as to the mechanism of photooxidation of cyt b_{559}, we subsequently focused our attention on the S_1 to S_2 state transition and studied the extent and rate of photooxidation of cyt b_{559} during continuous illumination in DCMU-treated PSII or after a single, saturating flash in untreated PSII. Clearly, the extent of photooxidation of cyt b_{559} depends on its own dark redox state and, in single-flash measurements, on the dark redox state of Q_A (since reaction centers with reduced Q_A prior to the flash are photochemically inactive). One significant complication of this measurement, in both the continuous illumination and single-flash experiments, is the spectral overlap of cyt b_{559} and C550, where the latter is the electrochromic shift of a pheophytin which linearly reflects the concentration of Q_A^- (van Gorkom, 1974a,b). Thus, in

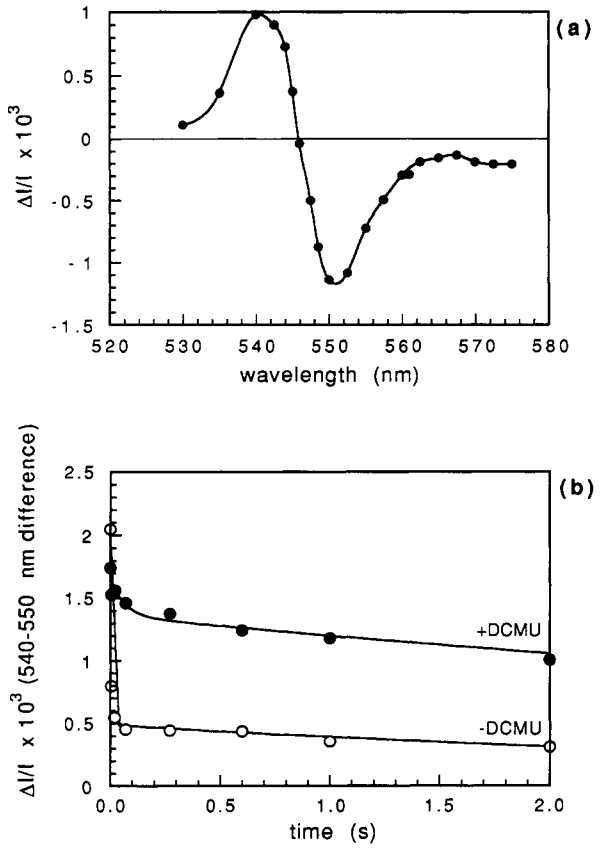

FIGURE 5: (a) Spectrum of the light-induced absorbance change 50 μs after a single, saturating flash in DCMU- (40 μM) and ferricyanide- (150 μM) treated PSII-enriched membranes at pH 8.0. (b) Time course of the flash-induced absorbance change of the 540–550-nm difference spectrum of dark-adapted PSII-enriched membranes in the absence (○) and presence (●) of 20 μM DCMU. The first data point was collected 500 μs after the actinic flash. The data are fit by a biexponential curve fit, where $t_{1/2}$ of the slow phase is 4.5 and 7.8 s in the absence and presence of DCMU, respectively (see text for further details).

order to determine the true rate of photooxidation of cyt b_{559} in O_2-evolving PSII, the contribution from C550 must be subtracted from the absorbance change at 560 nm.

Figure 5a shows the visible absorbance spectrum observed 50 μs after a single, saturating flash at room temperature in DCMU- and ferricyanide-treated PSII-enriched membranes. The absorbance maximum and minimum at 550 and 540 nm, respectively, are entirely consistent with the spectrum of C550 (van Gorkom, 1974b; Diner & Delosme, 1983). The spectral overlap of cyt b_{559} and C550 at short time points after the actinic flash is apparent in the comparison of the visible spectrum of cyt b_{559} (Figure 2) and C550 (Figure 5a). No correction was made for the contribution of C550 in Figures 2 and 4 owing to its small amplitude at 560 nm compared to that of cyt b_{559}.

In order to quantitate the dark redox state of Q_A, we subsequently determined the differential extinction coefficient for the 540–550-nm difference spectrum of C550. To calculate $\Delta\Delta\epsilon$ (540–550 nm), we induced the maximum photoreduction of Q_A by using 15 flashes (18 Hz) in PSII samples treated with 30 μM DCMU (to block Q_A to Q_B electron transfer) and 2 mM NH_2OH (to block Q_A^- oxidation by charge recombination). The absorbance change was measured for the 540–550-nm difference spectrum and at 325 nm (the reference wavelength of the Q_A^-–Q_A spectrum). The data were corrected for particle flattening [by the method of Duysens (1956) and Pulles et al. (1976)]. We have found a differential correction factor for particle flattening of 1.01 at 550 and 540 nm and

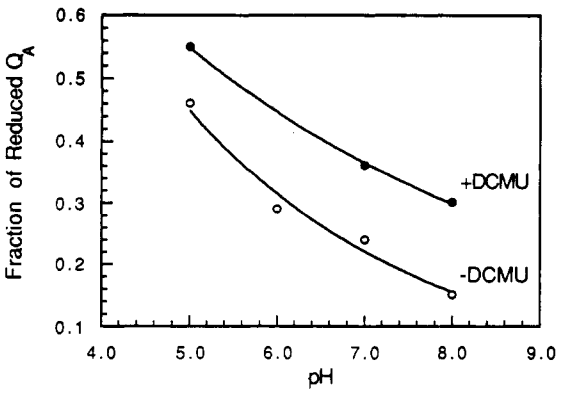

FIGURE 6: Fraction of reduced Q_A in dark-adapted PSII-enriched membranes in the absence (○) and presence (●) of 20 μM DCMU. The amount of Q_A^- was calculated from the value of $\Delta I/I$ of the 540–550-nm difference spectrum at 500 μs after the saturating flash [$\Delta\Delta\epsilon$ (540–550 nm) = 3.4 mM^{-1} cm^{-1} and 190 Chl per reaction center].

a factor of 1.08 and 325 nm in BBY-type PSII-enriched membranes [for further details see Buser et al. (1992)]. Using an extinction coefficient of 13 mM^{-1} cm^{-1} for the reduction of Q_A at 325 nm (van Gorkom, 1974b), we have calculated a differential extinction coefficient of 3.4 mM^{-1} cm^{-1} (540–550 nm) for the absorbance of C550. Our value of $\Delta\Delta\epsilon$ (540–550 nm) is in agreement with the previously reported reduced-minus-oxidized absorbance difference spectrum (corrected for particle flattening) of Q_A in Tris-washed, BBY-type PSII, where $\Delta\Delta\epsilon$ (540–550 nm) $\approx$ 3.7 mM^{-1} cm^{-1} (Dekker et al., 1984).

To determine the dark redox state of Q_A and the rate of reoxidation of photoreduced Q_A, we measured the photoinduced absorbance change of C550 after one saturating flash in untreated and DCMU-treated PSII (Figure 5b). A less than 2% decrease in the absorbance change of the 540–550-nm difference is observed between 50 and 500 μs after the actinic flash because of the slowed Q_A/Q_B electron transfer in BBY-type membranes [reviewed by Diner et al. (1991)]. The initial amplitude of the absorbance change of C550 (500 μs after the actinic flash) is attributed to the reaction centers in which Q_A is oxidized in the dark. Consistent with the mechanism of DCMU binding, a decrease in the amplitude of the 500-μs time point is observed upon addition of DCMU, corresponding to an increase in the fraction of dark-reduced Q_A (Lavergne & Etienne, 1980). The decay kinetics of photoreduced Q_A in Figure 5b are at least biexponential, both in the absence and in the presence of DCMU. In DCMU-treated PSII, the decay of the C550 absorbance change corresponds to recombination of the oxidized donor with Q_A^-. Assuming a model in which $S_n/Y_Z/P680$ are in equilibrium (Scheme I), the reoxidation of Q_A^- occurs via charge recombination of S_2 Q_A^-, $Y_Z^{\bullet}$ Q_A^-, and $P680^+$ Q_A^-. Since the $t_{1/2}$ values of $P680^+$ Q_A^- and $Y_Z^{\bullet}$ Q_A^- recombination are $\approx$900 μs and 10–400 ms (pH 5.0–7.5), respectively (Metz et al., 1989; Buser et al., 1990; Diner, unpublished results; Dekker et al., 1984), we assign the fast phase of the biexponential fit to the data for DCMU-treated PSII in Figure 5b to $P680^+$ Q_A^- and $Y_Z^{\bullet}$ Q_A^- recombinations and the slow phase to S_2 Q_A^- recombination.

Repeating the same type of measurement of C550 as shown in Figure 5b over the pH range 5–8, we subsequently determined the pH dependence of the dark redox state of Q_A and of the rate of Q_A^- reoxidation. Figure 6 shows the pH dependence of the amount of dark-reduced Q_A in untreated and DCMU-treated PSII-enriched membranes; in agreement with data from others (Lavergne & Etienne, 1980), we observe

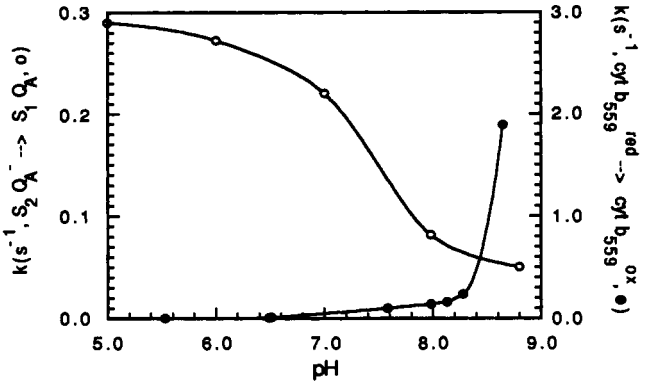

FIGURE 7: pH dependence of the rate of photooxidation of cyt b_{559} (●) in DCMU- (40 μM) treated PSII-enriched membranes during continuous illumination. For comparison, the kinetics for S_2 Q_A^- charge recombination (○) are also shown for DCMU- (20 μM) treated PSII samples. See text for further details concerning rate determinations.

an increase in the amount of dark-reduced Q_A with increasing acidity and upon addition of DCMU. The open circles of Figure 7 show the pH dependence of the rate of the slow phase of the biexponential fit to the C550 absorbance change in DCMU-treated PSII, where we have assigned the slow phase of Q_A^- reoxidation to S_2 Q_A^- recombination. Using fluorescence spectroscopy, Robinson and Crofts (1984) have found the same pH trend but a somewhat slower overall rate (by about a factor of 2) for S_2 Q_A^- recombination in pea chloroplasts.

Photooxidation of Cyt b_{559} during the S_1- to S_2-State Transition in O_2-Evolving PSII. With this information of the dark redox state and kinetics of Q_A, we can now begin to determine and analyze the rates and yields of photooxidation of cyt b_{559} observed during continuous illumination in DCMU-treated PSII and after a single, saturating flash in untreated PSII. Focusing on the data collected during illumination in Figure 3, we find that the time course of the absorbance change at 560 nm in DCMU-treated PSII-enriched membranes is not well fit by a single-exponential curve. Comparison of the absorbance change at 560 nm seen in the C550 spectrum (Figure 5a) and the cyt b_{559} time course (Figure 3) indicates that the reduction of Q_A, as reflected by C550, contributes approximately 10% to the initial rise in the absorbance change at 560 nm (pH 8.0). Using these results to deconvolute the contribution of C550, we have fit the time course of the absorbance change at 560 nm to a biexponential curve, where the initial fast phase (C550) was fixed to 10% of the total absorbance change at 560 nm. The second, slower phase (90% of the total absorbance change at 560 nm) was assigned to the photooxidation of cyt b_{559}. Figure 7 compares the pH dependence of the rate of photooxidation of cyt b_{559} during continuous illumination to the rate of S_2 Q_A^- recombination after a single flash in DCMU-treated PSII-enriched membranes. The maximum yield of photooxidation of cyt b_{559}, calculated from the total absorbance change at 560 nm, is tabulated as a function of pH in Table I. The rate (Figure 7) and extent (Table I) of photooxidation of cyt b_{559} during continuous illumination is small at pH < 6.0 and increases toward more basic pH, with a significant increase in the rate of photooxidation above pH 8.3.

Two significant observations from the continuous illumination data are that the extent of photooxidation of cyt b_{559} increases toward more basic pH and that C550 contributes to the absorbance change at 560 nm. With this information, we subsequently studied the yield of photooxidation of cyt b_{559} per saturating flash in O_2-evolving PSII-enriched membranes. Figure 8 presents a graphic description of the deconvolution method used to subtract the C550 contribution from the photooxidation kinetics of cyt b_{559} after one saturating flash at pH 8.0 (see legend to Figure 8 for further details). The deconvoluted kinetics of photooxidation of cyt b_{559} are fit well by a single-exponential curve, with $t_{1/2}$ = 540 ± 90 ms. The absolute absorbance change (shown in further detail in the inset of Figure 8) corresponds to the photooxidation of 4.7% of cyt b_{559}; under the conditions of this measurement (pH 8.0), 42% of cyt b_{559} is oxidized and 15% of Q_A is reduced in the dark prior to the actinic flash. As expected from our data of the photooxidation of cyt b_{559} observed during continuous illumination (Figures 4a and 7), we observe a decrease in the yield of photooxidation of cyt b_{559} after a single flash toward more acidic pH. Using the same deconvolution procedure as just described, we have found 2.5% of cyt b_{559} photooxidized after a single, saturating flash at pH 6.0, with $t_{1/2}$ = 760 ± 260 ms (data not shown). Of mechanistic importance, we find an increase in the yield per flash of photooxidation of cyt b_{559} toward basic pH concurrent with an increase in the lifetime of the S_2 Q_A^- charge separation (Figure 7). Assuming $P680^+$ is the oxidant to cyt b_{559} as shown in Scheme I, then this observation implies that $P680^+$ is in equilibrium with $Y_Z^\bullet$ and the Mn complex and that the rate and extent of photooxidation of cyt b_{559} are determined by the lifetime of the oxidizing equivalent on $S_n/Y_Z/P680$.

One essential question at this point is whether the observed photooxidation of cyt b_{559} originates from O_2-active or -inactive reaction centers. A comparison of the kinetics of cyt b_{559} photooxidation in untreated and NH_2OH-treated PSII-enriched membranes reveals significant differences in both the yields and rates of photooxidation in the presence and absence of the O_2-evolving complex. Figure 4a shows the pH dependence of the maximum yield of cyt b_{559} photooxidation observed during continuous illumination in both O_2-active and -inactive PSII samples. In contrast to the O_2-active PSII samples, the maximum yield of photooxidation of cyt b_{559} in O_2-inactive PSII-enriched membranes is virtually pH independent, and approximately 50% of cyt b_{559} is photooxidized in NH_2OH-treated samples during continuous illumination (in centers with ≈20% of dark-oxidized cyt b_{559} and ≈52–64% dark-reduced Q_A at pH 6.2). Furthermore, the yield per flash of cyt b_{559} photooxidation shows an opposite trend in untreated versus NH_2OH-treated PSII-enriched membranes over the pH range 5.0–8.0 (Table I). Not only are different yields of photooxidation observed, but the rate cyt b_{559} photooxidation is also significantly different in O_2-evolving versus non-O_2-evolving PSII preparations. The length of illumination necessary to obtain the maximum yield of photooxidation of cyt b_{559} in O_2-active and -inactive PSII samples is 21 and 1.8 s, respectively. Also, the rise time of the photooxidation of cyt b_{559} after a single flash is slower in O_2-evolving PSII preparations than in NH_2OH-treated samples: $t_{1/2}$ = 760 ± 260 ms (pH 6.0, data not shown) and 540 ± 90 ms (pH 8.0, Figure 8) in O_2-active PSII samples and $t_{1/2}$ = 10 ms (pH 5.0) and 13 ms (pH 6.0) in NH_2OH-treated PSII samples (Buser et al., 1990). These kinetic differences suggest that the flash-induced absorbance change at 560 nm in Figure 8 arises from the photooxidation of cyt b_{559} in reaction centers which form the S_2 Q_A^- (or S_2 Q_B^-) charge separation. Although O_2 evolution is known to be inhibited at basic pH in BBY-type PSII, Damoder and Dismukes (1984) have found the rate of formation and the yield of the S_2 state produced by single-flash excitation at room temperature or by continuous illumination at 200 K to be independent of pH over the pH range 5.5–8.5. It should

Table I

	O_2-Active PSII					
	$\Delta I/I_{max} \times 10^6$ (560 nm)[b]					
		cont illum			% Q_A^- in the dark[c,e]	
pH[a]	8 s after 1 flash (–DCMU)	–DCMU	+DCMU	% cyt b_{559}^{ox} in the dark[c,d]	–DCMU	+DCMU
5.0				85	46	55
5.5		1221 ± 369	670 ± 47	72		
6.0	332 ± 69			52	29	
6.5		1558 ± 355	1134 ± 169			
7.0				57	24	36
7.5		2628 ± 647	2559			
8.0	630 ± 165	3703 ± 328	2600 ± 417	42	15	30
8.5		4261	4332 ± 516	46		

	O_2-Inactive, NH_2OH-Treated PSII[f]		
	$\Delta I/I_{max} \times 10^6$ (560 nm)		
pH[a]	49 ms after 1 flash (–DCMU)	cont illum (–DCMU)	% Q_A^- in the dark[g] (–DCMU)
5.0	828 ± 122	6747 ± 23	43–55
5.5	625 ± 135	6145 ± 63	
6.0	627 ± 156	7501 ± 24	52–64
6.5	487 ± 193	7561 ± 24	
7.0	408 ± 99	7656 ± 98	
7.5	289 ± 60	7518 ± 90	

[a] The pH for these data is rounded to the nearest half pH unit. [b] 200 Chl/RC. [c] 190 Chl/RC. [d] The fraction of oxidized cyt b_{559} in dark-adapted PSII is taken from the data shown in Figure 1b. [e] The fraction of reduced Q_A in dark-adapted PSII in the absence and presence of DCMU is taken from the data shown in Figure 6. [f] The data for O_2-inactive, NH_2OH-treated PSII were taken from Buser et al. (1990) and corrected according to footnote 2 of this paper. [g] The fraction of reduced Q_A in dark-adapted, NH_2OH-treated PSII in the absence and presence of DCMU is taken from the data in Figure 6 in Buser et al. (1990), assuming 175 ± 25 chlorophylls per reaction center and $\Delta\Delta\epsilon$ (540–550 nm) = 3.4 mM^{-1} cm^{-1} for the measurement of C550.

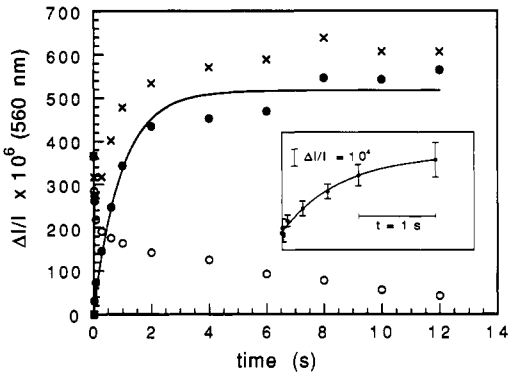

FIGURE 8: Time course of absorbance changes at 560 and at 550–540 nm. This figure provides a graphic description of the deconvolution method used to subtract the C550 contribution from the photooxidation kinetics of cyt b_{559} after a single, saturating flash in untreated PSII-enriched membranes (200 Chl/reaction center). The time course of the absorbance change at 560 nm (×) was corrected for the C550 contribution by scaling the 550–540-nm difference spectrum (○) to the initial time point at 50 μs after the actinic flash in the 560-nm difference spectrum. The resulting difference kinetics for cyt b_{559} (●), shown in further detail in the inset, are the average of seven experiments and are fit by a single-exponential curve with $t_{1/2}$ = 540 ms ± 90 ms.

be noted that all of these measurements are made in the presence of exogenous quinones (such as DCBQ or PPBQ), and it is not clear whether the pH dependence of O_2 evolution is due to the pH dependence of the O_2-evolving complex or to the electron-acceptor side (and the effectiveness of exogenous quinones to function as an electron acceptor at high pH). On the basis of these arguments, we conclude that the 4.7% photooxidation of cyt b_{559} observed in O_2-active PSII samples after a single flash at pH 8.0 occurs upon formation of the S_2 Q_A^- (or S_2 Q_B^-) charge separation.

Identification of the Reductant to Photooxidized Cyt b_{559} in O_2-Evolving PSII-Enriched Membranes. In our initial characterization of cyt b_{559} at pH 8.0, we observed not only the photooxidation but also the pH-dependent dark reduction of photooxidized cyt b_{559} in untreated O_2-evolving PSII (Figure 3). Clearly, the reducing equivalent for the reduction of oxidized cyt b_{559} must come from the electron-acceptor side of PSII; however, still unanswered is the identification of the reductant source, i.e., reduced Q_A, Q_B, or plastoquinol of the PQ pool. One significant observation from Figure 3 is the inhibition of the dark reduction of oxidized cyt b_{559} in the presence of DCMU. To further investigate this inhibition by DCMU, we measured both the dark reduction of cyt b_{559} and the photoreduction of the PQ pool at DCMU concentrations of 0, 3, and 10 μM. As before, the dark reduction of cyt b_{559} was monitored by the absorbance change at 560 nm after a period of continuous illumination. The photoreduction of the PQ pool was measured by the absorbance change at 265 nm, the minimum of the PQH_2 minus PQ difference spectrum. [We observed a red shift from 263 to 265 nm in the position of the minimum but the same width at half-height as compared to the PQH_2 minus PQ difference spectrum reported by Stiehl and Witt (1968) for spinach chloroplasts; data not shown.]

As shown in Figure 9a, the dark reduction of cyt b_{559} is significantly inhibited at 3 μM DCMU and completely blocked at 10 μM DCMU. We have determined an I_{50} of 0.19 μM (pH 8.0) for DCMU inhibition of the rate of dark reduction of photooxidized cyt b_{559} (data not shown). In contrast, the extent of reduction of the PQ pool is equivalent for DCMU concentrations of 0 and 3 μM and only somewhat inhibited at 10 μM DCMU, as seen in Figure 9b. In order to quantitate the PQ pool, we repeated the measurement in Figure 9b in a sample containing 40 μM DCMU, a concentration which completely blocks Q_A to Q_B electron transfer. Correcting the observed absorbance change for the fraction of Q_A which is reduced by electron transfer from Q_B^- to Q_A upon addition of DCMU (using the data in Figure 6) and correcting for particle flattening (see legend to Figure 9b), we find that the equivalent of 1 quinone, i.e., Q_A, is reduced in the presence of 40 μM DCMU (data not shown). Subtracting the contribution from Q_A in the measurement of Figure 9b, we find that 1.3 quinones are reduced during continuous illumination at concentrations of 0 and 3 μM DCMU and 0.65 quinone is reduced at 10 μM DCMU [$\Delta\epsilon$ (265 nm) = 13

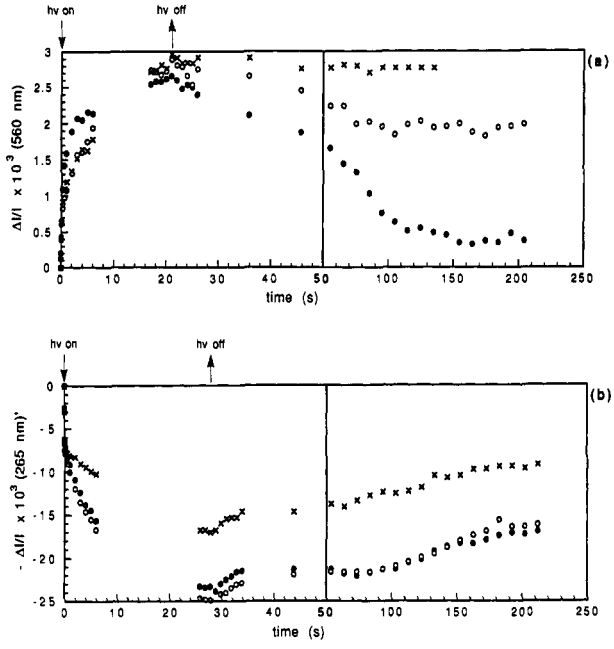

FIGURE 9: (a) Time course of the light-induced absorbance change at 560 nm in dark-adapted PSII treated with 0 (●), 3 (○), and 10 μM (×) DCMU at pH 8.0. (b) Time course of the light-induced absorbance change at 265 nm in dark-adapted PSII treated with 0 (●), 3 (○), and 10 μM (×) DCMU at pH 8.0. The ratio of Chl per reaction center was 190. The prime on $\Delta I/I$ (265 nm)′ denotes a correction for particle flattening, according to the method of Duysens (1956) and Pulles et al. (1976). We have determined a differential correction factor of 1.11 for the absorbance change at 265 nm in BBY-type PSII-enriched membranes [see Buser et al. (1992) for further details].

mM^{-1} cm^{-1}; Stiehl & Witt, 1968; Amesz, 1973]. In terms of Figure 9b, the initial fast absorbance change corresponds to the reduction of Q_A and the subsequent slower absorbance change observed during continuous illumination is due to the reduction of Q_B and a small PQ pool. The slow reduction of Q_B and the PQ pool may reflect either some modification of the Q_B site or a reduced PQ pool size in our BBY-type PSII preparations. Immediately after illumination, we observe a fast phase ($t_{1/2} \approx$ 1–5 s) in the recovery of the absorbance change at 265 nm (Figure 9b), most likely due to the reoxidation of a fraction of Q_A^-.

As Q_A is the most reduced at 10 μM DCMU while the rate of reduction of cyt b_{559} is lowered, it is clear that Q_A^- is not the reductant of cyt b_{559}^{ox}. Furthermore, since the extent of the reduction of Q_B and the PQ pool is the same after illumination at 0 and 3 μM DCMU while reduction of cyt b_{559} is slower at the latter concentration, it is unlikely that PQH_2 of the PQ pool is the direct source of reductant for the reduction of cyt b_{559}^{ox}. At 10 μM DCMU, there is a 50% inhibition of PQ reduction and the rate of cyt b_{559} reduction is significantly slowed. Altogether, these results are most consistent with reduced Q_B [Q_B^- •, Q_B^- •(H^+), Q_B^{2-}, Q_BH^-, or Q_BH_2] being the reductant to oxidized cyt b_{559} in O_2-evolving PSII-enriched membranes.

The interaction of cyt b_{559} and the Q_B site was further investigated by an acid-jump experiment, in which a drop in pH from 8.5 to 4.9 was induced by the addition of succinic acid in the absence and presence of DCMU (Figure 10). Because of the drift in the baseline induced by the addition of succinic acid, the acid-induced changes (±DCMU) at 560 nm were compared by taking the difference between the $\Delta I/I$ (560 nm) and that defined by a line connecting the $\Delta I/I$ at 555 and 565 nm (the wavelengths at half-height for the red-visible spectrum of cyt b_{559}). Similar experiments have been

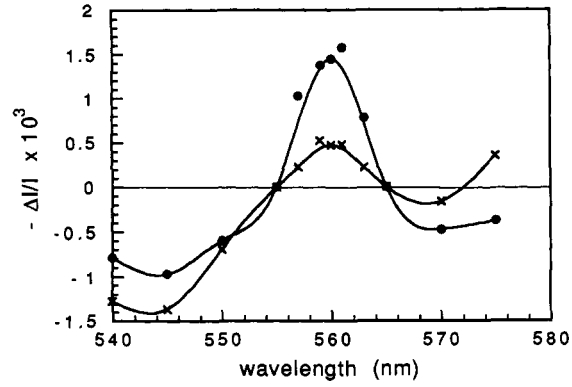

FIGURE 10: Alkaline minus acid difference spectrum measured 3 min after a pH jump from 8.5 to 4.9 in the absence (●) and presence (×) of 40 μM DCMU in PSII-enriched membranes (230 Chl per reaction center). The pH jump was achieved by the addition of 0.6 mM succinic acid to the sample in the absence of mediators.

reported before (Cramer et al., 1975; Horton et al., 1976); however, in contrast to the earlier studies, our measurements are made in the absence of redox mediators (such as ferricyanide/ferrocyanide), so that acid-induced changes of dark redox states directly represent changes of dark equilibria within PSII. In agreement with the pH dependence of the dark redox state of cyt b_{559} (Figure 1b), we observe the oxidation of ≈16% of cyt b_{559} at 3 min after dark acidification in the absence of DCMU. Furthermore, the acid-induced oxidation of cyt b_{559} is reversible upon addition of sodium hydroxide (data not shown). These results indicate that the pH dependence of the dark redox state of cyt b_{559}, shown in Figure 1b, is not just an artifact of the dark-adaption period.

If, as we suggest, reduced Q_B is the direct source of reductant to cyt b_{559}^{ox}, then we expect the binding of DCMU to modulate the acid-induced oxidation of cyt b_{559} by displacement of the endogenous occupant to the Q_B site (quinone, semiquinone, or quinol). A comparison of the absorbance difference between the amplitude at half-height (555–565 nm) and the amplitude at the maximum (560 nm) for cyt b_{559} in the absence and presence of 40 μM DCMU in Figure 10 indicates a 67% inhibition of the acid-induced oxidation of cyt b_{559} at 3 min after the acid jump. This result provides further support for a direct interaction between cyt b_{559} and Q_B. Assuming a dark equilibrium between cyt b_{559} and Q_B, one might expect the complete inhibition of the acid-induced oxidation of cyt b_{559} in the presence of excess DCMU. However, DCMU is found to only partially inhibit the oxidation of cyt b_{559} at early times after the addition of the acid (t = 3 min, Figure 10) and a slow increase in the extent of acid-induced oxidation is observed at longer timepoints. At 8 min after the addition of the acid, the oxidation of ≈31% and ≈20% of cyt b_{559} is observed in the absence and presence of DCMU (data not shown). The residual acid-induced oxidation of cyt b_{559} in the presence of DCMU may be explained by (a) a fraction of Q_B sites which do not bind DCMU effectively, (b) a thermodynamic change in the equilibrium state of the acceptor side induced by binding of DCMU, and/or (c) a kinetic effect involving competitive binding of DCMU and the quinone or semiquinone. The lattermost explanation appears most plausible, since the dissociation constant of DCMU (estimated from the I_{50} for the DCMU inhibition of the variable fluorescence, data not shown) is significantly greater in PSII-enriched membranes than in chloroplasts (Stein et al., 1984), which may allow for competitive DCMU and semiquinone binding to the Q_B site in PSII samples. In any case, the main point of Figure 10 is that, in the absence of exogenous mediators, DCMU affects the acid-induced oxidation of cyt

b_{559}, suggesting a dark equilibrium between cyt b_{559} and Q_B in untreated PSII-enriched membranes.

DISCUSSION

Several earlier reports have suggested cyt b_{559} mediates a cyclic pathway for electron transfer around PSII (Cramer & Whitmarsh, 1977; Heber et al., 1979; Arnon & Tang, 1988; Thompson & Brudvig, 1988). However, the paths of its oxidation and reduction have remained controversial, in part, due to the lack of kinetic characterization of cyt b_{559} under physiological conditions. We previously proposed a model for electron transfer in PSII (Scheme I) based on data pertaining to the photooxidation of cyt b_{559} and Y_D in O_2-inactive PSII-enriched membranes (Buser et al., 1990). Since cyt b_{559} and Y_D are efficiently photooxidized in both Mn-depleted PSII-enriched membranes and in a mutant of *Synechocystis* PC 6803 lacking Y_Z (Metz et al., 1989; Diner, unpublished results), we favor a model in which $P680^+$ is the direct oxidant of cyt b_{559} and Y_D. The important aspect of this model is that S_{n+1}, $Y_Z^{\bullet}$, and $P680^+$ are in redox equilibrium and cyt b_{559} and Y_D are oxidized via $P680^+$. This model predicts that the photooxidation of cyt b_{559} and Y_D occurs within the lifetime of the oxidizing equivalent on the donor side of the PSII reaction center. Consistent with this prediction, the rates of photooxidation of cyt b_{559} after a single flash (Figure 8) and of $S_2\,Q_A^-$ recombination (Figure 7) are of the same order of magnitude. As expected, when the two rates cross over and the rate of cyt b_{559} oxidation becomes faster than the rate of $S_2\,Q_A^-$ recombination, then the extent of photooxidation of cyt b_{559} increases significantly. Similarly, the rate of photooxidation of Y_D is also of the same order of magnitude, and the rate and yield of the photooxidation of Y_D exhibit the same trend in pH as the photooxidation of cyt b_{559} ($t_{1/2}$ = 10 and 1 s at pH 6 and 8, respectively; Vass & Styring, 1991).

Whereas we have found the yield and rate of photooxidation of cyt b_{559} in O_2-evolving PSII-enriched membranes to increase toward more basic pH (Figures 4a and 7), Horton and Cramer (1976) have observed an opposite trend in chloroplast preparations, where the yield of photooxidation of cyt b_{559} increases with increasing acidity. However, it is difficult to compare our results from PSII-enriched membranes to their results in chloroplasts due to the inherent difference in the two preparations and the very different experimental conditions. Two factors which complicate such pH measurements in thylakoid or chloroplast preparations are the membrane potential and the buffering capacity of the membrane itself, such that the pH inside the thylakoid vesicle is most likely not the same as the pH of the buffer. Another significant problem in optical measurements of cyt b_{559} is the deconvolution of absorbance changes of cytochromes *f* and b_6 from the α-band of cyt b_{559} in thylakoids (Buser et al., 1992).

In the dark period following continuous illumination, we have observed the dark rereduction of photooxidized cyt b_{559}, where the extent and rate of reduction decreases with decreasing pH and appears to be inhibited at pH < 6.4 (Figure 4b). Although the dark reduction kinetics of cyt b_{559} have not been previously reported in PSII-enriched membranes, Whitmarsh and Cramer (1977) have reported the photoreduction of cyt b_{559} in chloroplasts. Similar to our results in PSII-enriched membranes, the kinetics of photoreduction of cyt b_{559} decrease toward more acidic pH in chloroplasts. These authors report a plateau in the maximum of the extent of photoreduction of cyt b_{559} between pH 6.5 and 8.0 and a maximum in the rate at pH 8.5 (Whitmarsh & Cramer, 1978). Although the reduction kinetics of cyt b_{559} exhibit a similar pH dependence in chloroplast and PSII-enriched membranes, the rate of reduction is almost 3 orders of magnitude faster in chloroplasts ($t_{1/2}$ = 100 ± 10 ms at pH 7.8; Whitmarsh & Cramer, 1977) than in BBY-type PSII ($t_{1/2} \approx 70$ s at pH 7.8; this study). The difference in the rate of cyt b_{559} reduction may be attributed to a higher concentration of quinol and possibly a more intact Q_B site in the chloroplast preparation as compared to the BBY-PSII preparation.

Whitmarsh and Cramer (1978) also investigated the reductive path for cyt b_{559} by comparing the extent of photoreduction of cyt b_{559} to the steady-state relative Chl fluorescence yield as a function of DCMU. In their study, the increase in the fluorescence yield at increasing concentrations of DCMU was directly correlated to the number of blocked PSII reaction centers. Nearly 7 times as much DCMU was found necessary to inhibit 50% of the photoreduction of cyt b_{559} (1.5 μM) as was needed to cause a 50% increase in the maximum fluorescence yield (0.22 μM). On the basis of these results, Whitmarsh and Cramer (1978) concluded that cyt b_{559} was photoreduced after an electron-sharing pool in chloroplasts. Using a similar somewhat more direct approach, we measured the dark reduction of cyt b_{559} (Figure 9a) and the photoreduction of the PQ pool (Figure 9b) as a function of DCMU concentration in PSII-enriched membranes at pH 8.0. Our results show that, even at low DCMU concentrations (3 μM), the reduction path for oxidized cyt b_{559} is largely inhibited while the PQ pool can still be completely reduced during continuous illumination (Figure 9)—suggesting that neither the reduced PQ pool nor Q_A^- is the direct reductant to oxidized cyt b_{559}. Collectively, our data are most consistent with reduced Q_B as the direct reductant source to cyt b_{559}^{ox}:

$$\text{cyt } b_{559}^{ox}\,Q_BH_2 \overset{K_{eq}}{\rightleftharpoons} \text{cyt } b_{559}^{red}\,Q_B^{-}{}^{\bullet}(H^+) + H^+ \qquad (1)$$

where, in the proposed equilibria, $K_{eq} > 1$ at basic pH and <1 at acidic pH. Both the pH dependence of the dark redox state of cyt b_{559} (Figure 1b) and Q_B (Figure 6 and text), as well as the acid-induced oxidation of cyt b_{559} (Figure 10), support this equilibrium. The measurement in Figure 9 also tends to support the equilibrium in (1), since the charge-separated state immediately after continuous illumination is cyt $b_{559}^{ox}\,Q_BH_2$. Although we cannot exclude the reduction of cyt b_{559}^{ox} by $Q_B^{-}{}^{\bullet}$ from our experimental data, we can obtain more insight from a comparison of the midpoint potentials of cyt b_{559}^{ox}/cyt b_{559}^{red} to the redox couples $Q_B/Q_B^{-}{}^{\bullet}$, $Q_B^{-}{}^{\bullet}/Q_BH_2$, and Q_B/Q_BH_2. Taking at least 45% of the cyt b_{559} to be high potential and pH independent ($E_{m,pH\text{-}indep.}$ = 380 mV; Ortega et al., 1988; Thompson et al., 1989), we find that the midpoint potentials of both $Q_B/Q_B^{-}{}^{\bullet}$ and Q_B/Q_BH_2 are more negative than that of high-potential cyt b_{559}^{ox}/cyt b_{559}^{red} over the pH range 4–9 [for review of acceptor-side midpoint potentials see Diner et al. (1991)]. Taking into account a pK_a of 7.9 for $Q_B^{-}{}^{\bullet}/Q_B^{-}{}^{\bullet}(H^+)$ (Robinson & Crofts, 1984), only the midpoint potential of $Q_B^{-}{}^{\bullet}/Q_BH_2$ ($E_{m,7}$ = 290 mV) is more positive at acidic pH (e.g., $E_{m,4.9} \approx 420$ mV) and more negative at basic pH (e.g., $E_{m,8.5} \approx 170$ mV) than that of high-potential cyt b_{559}^{ox}/cyt b_{559}^{red} with a cross-over point between pH 5 and 6. From these thermodynamic considerations, only the redox couple $Q_B^{-}{}^{\bullet}/Q_BH_2$ may be in redox equilibrium with high-potential cyt b_{559}^{ox}/cyt b_{559}^{red}, such that Q_BH_2 can reduce cyt b_{559}^{ox} only at elevated pH. Such reduction would be enhanced further at alkaline pH (consistent with our observations) if one takes into consideration lower potential forms of cyt b_{559} ($E_{m,>7.6}$ = 145 mV; Ortega et al., 1988). From the experimental data and this thermodynamic analysis, we argue in favor of Q_BH_2 as the source of reductant of cyt b_{559}^{ox}, although further experiments

Scheme II: Summary of Pathways and Rates of Electron Donation to P680[a]

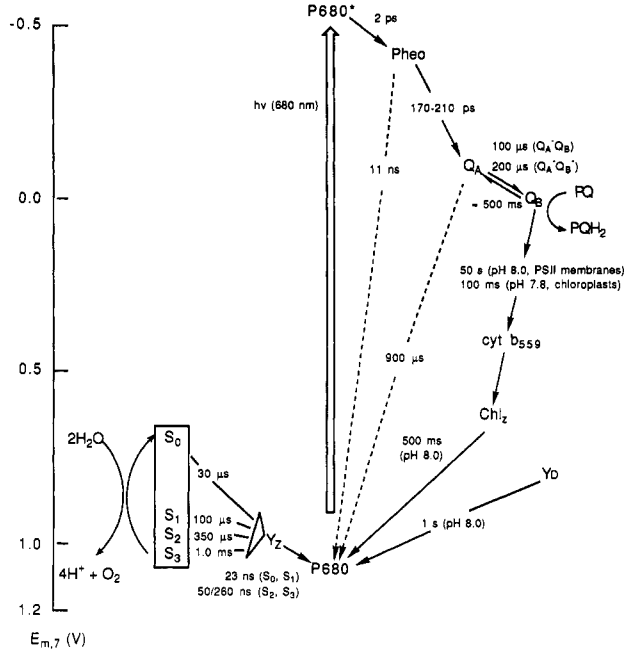

[a] Rates are written in terms of $t_{1/2}$. Solid lines, forward electron transfer reactions; dotted lines, reverse charge recombination reactions [reviewed in Cramer and Whitmarsh (1977), Babcock (1987), Thompson et al. (1988), Vass and Styring (1991), and Diner et al. (1991)].

will be necessary to unequivocally show whether the quinol or the semiquinone, or both, is the direct reductant to cyt b_{559}^{ox}.

On the basis of our results and their mechanistic implications, we can now incorporate the paths of oxidation and reduction of cyt b_{559} in the overall schematic picture of electron transfer in PSII (Scheme II). As shown, cyt b_{559} mediates cyclic transfer within PSII, where cyt b_{559} is oxidized by $P680^+$ via a monomer chlorophyll (Chl_z; Thompson et al., 1988) and is reduced by a reducing equivalent from the Q_B site. In the past, our laboratory has suggested that the cyt b_{559} path functions to protect PSII from photoinhibition by rereducing $P680^+$ either when the dominant Mn path is inhibited or when the O_2-evolving enzyme is unable to maintain the electron requirement of the primary electron donor under continuous high-intensity light conditions (Thompson & Brudvig, 1988). Under physiological conditions, reduction of $P680^+$ proceeds primarily along the Mn path and, to a much lesser extent, along the cyt b_{559} and Y_D paths. During strong-light illumination, the inhibition of the S_1 to S_2 state transition and the stable oxidation of cyt b_{559} (and Y_D) are observed; only the monomer Chl_z of the cyt b_{559} path remains photochemically active and is not stably oxidized during periods of high-intensity illumination (Styring et al., 1990). Although the origin of photoinhibition remains controversial and different schemes involving donor- or acceptor-side phenomena have been reported [reviewed by Osmond (1981) and Powles (1984)], any mechanism which may protect PSII from photoinhibition must involve the dissipation of excess excitation energy before the occurrence of irreversible, damaging reactions. The cyt b_{559} path may offer this protection in one of two ways. One possibility is that the cyt b_{559} cycle around PSII is sufficient to rereduce $P680^+$ under photoinhibitory conditions in the in vivo system. Although the reduction kinetics of cyt b_{559} in BBY-type PSII-enriched membranes are too slow for such a model, the rate of reduction of cyt b_{559} is more than 2 orders of magnitude faster in chloroplasts ($t_{1/2}$ = 100 ms; Whitmarsh & Cramer, 1977) than in PSII-enriched membranes and is of the same magnitude as the turnover rate in saturating light. In this case, the observation that cyt b_{559} is stably oxidized under such conditions would mean that the rate of cyt b_{559} to Chl_z^+ electron donation is faster than the rate of cyt b_{559} reduction. A second possibility by which the cyt b_{559} path may protect PSII from photoinhibition involves fluorescence quenching. In this case, Chl_z^+, formed by electron donation to $P680^+$, quenches excitation energy by radiationless decay of the excited doublet to the ground state while cyt b_{559} remains oxidized. In accordance with the latter mechanism of energy dissipation, an increase in the quenching of Chl fluorescence together with a decrease in the efficiency of electron transport is observed as the light intensity is increased and at low pH (Noctor & Horton, 1990). Recently, Crofts and Horton (1991) have found that the low-pH-dependent quenching of Chl fluorescence also requires oxidizing conditions, where redox titrations indicated that a component with a midpoint potential of 405 mV at pH 4.0 needed to be oxidized in order to observe quenching of Chl fluorescence.

Clearly, our data on the photooxidation and dark reduction of cyt b_{559} together with information on the dark redox state of cyt b_{559} and Q_A (and indirectly also Q_B) have significant implications on the predicted dark redox state of PSII and, as such, on the interpretation and simulation of flash-induced thermoluminescence, flash-induced O_2 yield patterns and other PSII-related reactions. For example, in the past, the charge-separated state $S_2\,Q_A\,Q_B^{2-}$ cyt b_{559}^{ox} was assumed not to show thermoluminescence due to protonation and dissociation of Q_BH_2 (Rutherford et al., 1984). However, electron transfer from bound Q_BH_2 to oxidized cyt b_{559} would result in the state $S_2\,Q_A\,Q_B^-\,\cdot$ cyt b_{559}^{red}, which would be expected to show thermoluminescence due to $S_2\,Q_B^-\,\cdot$ charge recombination. Knowing the pH dependence of the dark reduction of cyt b_{559}, reduction of cyt b_{559} by $Q_B^-\,\cdot$ could be further examined by studying the thermoluminescence of PSII-enriched membranes after 1 and 2 flashes with and without cyt b_{559} preoxidized over the pH range 5–8.

It is interesting to note that the pH dependence of the kinetics of photooxidation and dark reduction of cyt b_{559} in PSII-enriched membranes may explain the one-flash shift observed in the period 4 oscillation of O_2 release at basic pH. Plijter et al. (1986) observed that the release of O_2 is shifted to the fourth flash at pH ≥ 7.5 in BBY-type PSII preparations (time between flashes = 300 ms). The authors ascribe the one-flash shift to the dark reduction of the S_1 state to S_0 at basic pH. Although their experimental conditions are somewhat different, we would like to suggest an alternative explanation to their data. The pH at which the release of O_2 is shifted from the third to the fourth flash corresponds quite well to the pH dependence of the kinetics of cyt b_{559} photooxidation (Figure 7). On the time scale between their flashes, it is possible that cyt b_{559} is oxidized after the first, second, or third flash at pH > 7.5, thereby reducing S_{n+1} to S_n and shifting the O_2 release pattern by one flash. Furthermore, Plijter et al. (1986) report a halftime of 45 s for the rate of reduction of S_1 to S_0 at pH 8.3. Entirely consistent with our reinterpretation of their observations, we observe a $t_{1/2}$ = 35 s for the rate of reduction of cyt b_{559} at pH 8.3 (Figure 4b). Therefore, we suggest that, at basic pH and for a relatively slow flash frequency, a one-flash shift in the four-flash periodicity of the O_2 release may be due not to a change in the dark S-state population but instead to the rereduction of S_{n+1} to S_n after the first, second, or third flash by cyt b_{559}. In agreement with our reinterpretation, Damoder and Dismukes (1984) have found the yield of formation of the S_2 state after

a single flash at room temperature to be independent of pH, indicating a pH-independent dark S-state population.

Most likely, the reason the photooxidation of cyt b_{559} has not been observed previously in O_2-evolving PSII is due to the significant fraction of stable, oxidized cyt b_{559} in the dark (Figure 1b) and its slow rate of photooxidation (Figure 7) at pH 6.0. Similar to the redox characterization of cyt b_{559} in PSII by Ortega et al. (1988), we find the fraction of dark-oxidized cyt b_{559} is pH independent at neutral and basic pH (with about $^1/_3$ of cyt b_{559} oxidized in dark-adpated PSII-enriched membranes) but becomes pH dependent at more acidic pH. These authors assume a stoichiometry of two cyt b_{559} per reaction center and interpret their redox titration data of cyt b_{559} in terms of two distinct populations, a low- and a high-potential form of cyt b_{559}. However, our data from optical and EPR spectroscopy (Buser et al., 1992; Figure 1) indicate a 1:1 stoichiometry of cyt b_{559} per PSII reaction center. Assuming one copy of cyt b_{559} per reaction center, the obvious question is the physiological significance of the range of observed midpoint potential(s) of cyt b_{559}. Unfortunately, most redox titration studies of cyt b_{559} and also of other redox-active components of PSII are usually performed on dark-adapted PSII-enriched membranes or thylakoids, which may not be representative of the redox state of the sample during illumination. As a result, it is difficult to correlate the dark-oxidized and the photooxidized fractions of cyt b_{559} to a specific potential form. To understand the significance of the different potential forms of cyt b_{559}, it is necessary to determine the redox potential of cyt b_{559} and the electron acceptors Q_A and Q_B as a function of pH and to correlate these data with the photochemical reactions of cyt b_{559}. Such a potentiometric redox titration would provide additional information on the equilibrium between cyt b_{559} and Q_B, as shown in eq 1, and should yield a consensus regarding the function of the different forms of cyt b_{559}.

REFERENCES

Amesz, J. (1973) *Biochim. Biophys. Acta 301*, 35.
Arnon, D. I. (1949) *Plant Physiol. 24*, 1.
Arnon, D. I., & Tang, G. M.-S. (1988) *Proc. Natl. Acad. U.S.A. 85*, 9524.
Babcock, G. T. (1987) in *Photosynthesis* (Amesz, J., Ed.) p 125, Elsevier Science Publishers, The Hague, The Netherlands.
Babcock, G. T., Ghanotakis, D. F., Ke, B., & Diner, B. A. (1983) *Biochim. Biophys. Acta 723*, 276.
Beck, W. F., de Paula, J. C. & Brudvig, G. W. (1985) *Biochemistry 24*, 3035.
Ben-Hayyim, G. (1984) *Eur. J. Biochem. 106*, 329.
Berthold, D. A., Babcock, G. T., & Yocum, C. F. (1981) *FEBS Lett. 134*, 231.
Buser, C. A., Thompson, L. K., Diner, B. A., & Brudvig, G. W. (1990) *Biochemistry 29*, 8977.
Buser, C. A., Diner, B. A., & Brudvig, G. W. (1992) *Biochemistry* (preceding paper in this issue).
Conjeaud, H., & Mathis, P. (1980) *Biochim. Biophys. Acta 590*, 353.
Cramer, W. A., & Whitmarsh, J. (1977) *Annu. Rev. Plant Physiol. 28*, 133.
Cramer, W. A., Horton, P., & Wever, R. (1975) in *Electron Transfer Chains and Oxidative Phosphorylation* (Quagliariello, E., Ed.) p 31, North-Holland Publishing Co., Amsterdam, The Netherlands.
Cramer, W. A., Theg, S. M., & Widger, W. R. (1986) *Photosynth. Res. 10*, 393.
Crofts, J., & Horton, P. (1991) *Biochim. Biophys. Acta 1058*, 187.
Damoder, R., & Dismukes, G. C. (1984) *FEBS Lett. 173*, 157.
Dekker, J. P., van Gorkom, H. J., Brok, M., & Ouwehand, L. (1984) *Biochim. Biophys. Acta 765*, 301.
Diner, B. A., & Delosme, R. (1983) *Biochim. Biophys. Acta 722*, 452.
Diner, B. A., Petrouleas, V., & Wendoloski, J. J. (1991) *Physiol. Plant. 81*, 423.
Duysens, L. N. M. (1956) *Biochim. Biophys. Acta 19*, 1.
Heber, U., Kirk, M. R., & Boardman, N. K. (1979) *Biochim. Biophys. Acta 546*, 292.
Horton, P., & Cramer, W. A. (1976) *Biochim. Biophys. Acta 430*, 122.
Horton, P., Whitmarsh, J., & Cramer, W. A. (1976) *Arch. Biochem. Biophys. 176*, 519.
Joliot, P., Béal, D., & Frilley, B. (1980) *J. Chim. Phys. 77*, 209.
Lavergne, J. (1987) *Biochim. Biophys. Acta 894*, 91.
Lavergne, J., & Etienne, A.-L. (1980) *Biochim. Biophys. Acta 593*, 136.
Mathis, P., & Rutherford, A. W. (1987) in *Photosynthesis* (Amesz, J., Ed.) p 63, Elsevier Science Publishers B. V., The Hague, The Netherlands.
Metz, J. G., Nixon, P. J., Rögner, M., Brudvig, G. W., & Diner, B. A. (1989) *Biochemistry 28*, 6960.
Noctor, G., & Horton, P. (1990) *Biochim. Biophys. Acta 1016*, 228.
Ortega, J. M., Hervás, M., & Losada, M. (1988) *Eur. J. Biochem. 171*, 449.
Osmond, C. B. (1981) *Biochim. Biophys. Acta 639*, 77.
Pakrasi, H. B., Nyhus, K. J., & Granok, H. (1990) *Z. Naturforsch. 45C*, 423.
Plijter, J. J., de Groot, A., van Dijk, M. A., & van Gorkom, H. J. (1986) *FEBS Lett. 195*, 313.
Powles, S. B. (1984) *Annu. Rev. Plant Physiol. 35*, 15.
Pulles, M. P. J., van Gorkom, H. J., & Verschoor, G. A. M. (1976) *Biochim. Biophys. Acta 440*, 98.
Robinson, H. H., & Crofts, A. R. (1984) in *Advances in Photosynthesis Research* (Sybesma, C., Ed.) Vol. 1, p 477, Martinus Nijhoff/Dr. W. Junk Publishers, The Hague, The Netherlands.
Rutherford, A. W., Renger, G., Koike, H., & Inoue, Y. (1984) *Biochim. Biophys. Acta 767*, 548.
Samson, G., & Fork, D. C. (1991) *Photosynth. Res. 27*, 179.
Stein, R. R., Castellvi, A. L., Bogacz, J. P., & Wraight, C. A. (1984) *J. Cell. Biochem. 24*, 243.
Stiehl, H. H., & Witt, H. T. (1968) *Z. Naturforsch. 23b*, 220.
Styring, S., Virgin, I., Ehrenberg, A., & Andersson, B. (1990) *Biochim. Biophys. Acta 1015*, 269.
Thompson, L. K., & Brudvig, G. W. (1988) *Biochemistry 27*, 6653.
Thompson, L. K., Miller, A.-F., de Paula, J. C., & Brudvig, G. W. (1988) *Is. J. Chem. 28*, 121.
Thompson, L. K., Miller, A.-F., Buser, C. A., de Paula, J. C., & Brudvig, G. W. (1989) *Biochemistry 28*, 8048.
Tsujimoto, H. Y., & Arnon, D. I. (1985) *FEBS Lett. 179*, 51.
van Gorkom, H. J. (1974a) *Biochim. Biophys. Acta 347*, 417.
van Gorkom, H. J. (1974b) *Biochim. Biophys. Acta 347*, 439.
Vass, I., & Styring, S. (1991) *Biochemistry 30*, 830.
Whitmarsh, J., & Cramer, W. A. (1977) *Biochim. Biophys. Acta 460*, 280.
Whitmarsh, J., & Cramer, W. A. (1978) *Biochim. Biophys. Acta 501*, 83.
Yamagishi, A., & Fork, D. C. (1987) *Arch. Biochem. Biophys. 259*, 124.

Registry No. cyt b_{559}, 9044-61-5; Chl P680, 53808-91-6.